Journal of Maps

ISSN: 1744-5647 (Online) Journal homepage: www.tandfonline.com/journals/tjom20

Submerged coastal systems along the western Sardinian shelf (Mediterranean Sea)

Claudio Kalb, Duccio Bertoni, Annelore Bezzi, Giulia Casagrande, Alessandro Conforti, Giacomo Deiana, Giorgio Fontolan, Marco Frau, Antonio Funedda, Davide Martinucci, Paolo Emanuele Orrù, Simone Simeone & Giovanni De Falco

To cite this article: Claudio Kalb, Duccio Bertoni, Annelore Bezzi, Giulia Casagrande, Alessandro Conforti, Giacomo Deiana, Giorgio Fontolan, Marco Frau, Antonio Funedda, Davide Martinucci, Paolo Emanuele Orrù, Simone Simeone & Giovanni De Falco (2025) Submerged coastal systems along the western Sardinian shelf (Mediterranean Sea), Journal of Maps, 21:1, 2474831, DOI: 10.1080/17445647.2025.2474831

To link to this article: https://doi.org/10.1080/17445647.2025.2474831

JOURNAL OF MAPS
2025, VOL. 21, NO. 1, 2474831
https://doi.org/10.1080/17445647.2025.2474831

Taylor & Francis
Taylor & Francis Group

OPEN ACCESS Check for updates

Submerged coastal systems along the western Sardinian shelf (Mediterranean Sea)

Claudio Kalb [a], Duccio Bertoni [b], Annelore Bezzi [c], Giulia Casagrande [c], Alessandro Conforti [a], Giacomo Deiana [d], Giorgio Fontolan [c], Marco Frau [d], Antonio Funedda [d], Davide Martinucci [c], Paolo Emanuele Orrù [d], Simone Simeone [a] and Giovanni De Falco [a]

[a]CNR-IAS – Istituto per lo studio degli impatti Antropici e Sostenibilità in ambiente marino, Oristano, Italy; [b]Dipartimento di Scienze della Terra, University of Pisa, Pisa, Italy; [c]Dipartimento di Matematica e Geoscienze, University of Trieste, Trieste, Italy; [d]Dipartimento di Scienze Chimiche e Geologiche, University of Cagliari, Cagliari, Italy

ABSTRACT
This paper presents the geophysical mapping of the western Sardinia continental shelf (Mediterranean Sea, Italy). The focus is to highlight the various submerged coastal systems associated with the last eustatic cycle, consisting of beach barriers, submerged depositional terraces, submerged dunes and the current infralittoral prograding wedges. The study was carried out by interpreting MBES data, SSS photomosaics, reflection seismic data and aerial orthophotos, validated by sediment sampling. All data were processed to produce a 1:100,000 scale map showing a wide sector of the western Sardinian shelf and summarising the morphological and sedimentological features. The formation and evolution of the submerged coastal systems have been related to the available models of the last sea-level rise from the LGM to the present day, denoting a pulse pattern at sea-level change mainly triggered by northern hemisphere meltwater pulses. Furthermore, the map shows the general distribution of sediments, marine phanerogam meadows and rocky outcrops.

ARTICLE HISTORY
Received 4 December 2024
Revised 20 February 2025
Accepted 27 February 2025

KEYWORDS
Submarine depositional terrace; Barriers; Sea-level rise; Meltwater pulses

1. Introduction

Late Quaternary coastal systems that migrate landward as sea level rises have been described in several sites over transgressive continental shelves (Budillon et al., 2022; Chiocci & Orlando, 1996; De Falco et al., 2015b). The present-day infralittoral coastal systems extend between the shoreface and the inner continental shelf, from the mean storm wave base to the mean fair-weather wave base (Reading & Collison, 1996). Several studies have evaluated various morphologies that characterise the present-day beach systems, focusing on the submerged beach, such as infralittoral prograding wedges (IPWs) (Budillon et al., 2022; Chiocci & Orlando, 1996; Field & Roy, 1984; Hernández-Molina et al., 2000). These prograding sediment wedges develop under the combined action of storm waves and downwelling or cross-shore currents that redistribute littoral sediments below the depth of closure (Hernández-Molina et al., 2000). During storms, sediments are transported downslope beyond the storm-wave base, where their preservation potential increases with depth. The terraced surface grows in parallel with the progradation of the external clinoforms, and its edge depth depends on offshore accommodation space, sea level stability over time, and the frequency and intensity of extreme sea storms (Fernàndez-Salas et al., 2009; Hampson & Storms, 2003). Although the IPW's growth is mainly related to modern sea level, the conceptual model of their formation can work as an analogy for deeper submerged terraces, formed on the middle and outer shelf during past lower sea levels (Budillon et al., 2022). Past examples of these depositional bodies, commonly referred to as 'low-stand submerged depositional terraces' (Casalbore et al., 2018; Chiocci & Orlando, 1996; Romagnoli, 2004), have been recognised worldwide, both on land in Pleistocene successions (Massari & Chiocci, 2006; Pomar & Tropeano, 2001) and in deep water along the shelf profile (Budillon et al., 2012; Chiocci & Romagnoli, 2004; Firetto Carlino et al., 2012; Pepe et al., 2014). Recent studies on the western Sardinian shelf (Brambilla et al., 2019; Conforti et al., 2016; De Falco et al., 2010; De Falco et al., 2015a; De Falco et al., 2015b) show several features in accordance with the above-mentioned concepts.

During the last eustatic cycle, following the Last Glacial Maximum (LGM), sea level has risen by

CONTACT Claudio Kalb claudio.kalb@ias.cnr.it Istituto per lo Studio degli Impatti Antropici e la Sostenibilità in Ambiente Marino - Consiglio Nazionale delle Ricerche (CNR-IAS), Sede Secondaria, Località Sa Mardini 09170, Torregrande (OR), Italy
Supplemental data for this article can be accessed online at https://doi.org/10.1080/17445647.2025.2474831.

about 125 m (Deiana et al., 2021; Lambeck et al., 2014; Lambeck & Bard, 2000; Liu & Milliman, 2004), reaching a near stillstand in the Mediterranean around ~4000 yr BP (Vacchi et al., 2021). Consequently, the submerged depositional terraces (SDTs), found in the study area, can be traced back to past IPWs of the coastal system. At the same time, morphologies such as barriers can be associated with them related to past shorelines. Thus, both morphologies can be linked with stillstands or slow rises in sea level since the LGM, about 24–21 ka BP, and during the post-LGM transgression, making them relicts. In fact, many authors have identified a nonlinear and variable trend in past glacial sea-level rise (SLR). This variability is attributed to climate changes that alternated phases of rapid glacier melt, characterised by accelerated SLR, known as meltwater pulses (MWPs), with phases of slower, progressive phases of slower glacier melt (Blanchon, 2011; Fairbanks, 1989; Lambeck et al., 2004, 2011; Liu & Milliman, 2004; Velay-Vitow et al., 2024). Furthermore, in the northern hemisphere the MWPs are linked with the lake drainage and not directly by the glacier melt (Gregoire et al., 2012; Harrison et al., 2019; Smith et al., 2011). In addition, the rate of sea-level rise decreased in the central and western Mediterranean from 8.7 ± 0.9 mm per year to 3.1 ± 0.8 mm per year during the period 8000–5000 yr BP (Vacchi et al., 2021). Consequently, the SDTs and barriers can be traced back to the stillstand phases of SLR in the Mediterranean area, that followed the MWPs (Casalbore et al., 2018; Zecchin et al., 2015).

The objective of this work is to map the submerged coastal systems, including coastal barriers, submerged depositional terraces, paleo-cliffs and dunes, present along the continental shelf of central-western Sardinia. In particular, the specific aim is to relate the distribution, depth and morphology of submerged coastal systems to variations in the rate of sea-level rise correlated with MPWs. Results of this mapping are shown in the main map.

2. Study area

The study is focused on the western shelf of Sardinia. Sardinia is the second largest island of the Mediterranean Sea, with an area of ~24,000 km^2 and ~2000km of coastline length (main map). The continental shelf of the western Sardinia is 5–40 km wide and is characterised by different morphological domains controlled by tectonic features (Carboni et al., 1989; Conforti et al., 2016; De Falco et al., 2015a; Fais et al., 1996; Geletti et al., 2014; Sage et al., 2005).

Along the mid-shelf of the study area, the Paleozoic-Early Miocene acoustic basement rises and outcrops. Along the inner shelf, a sedimentary basin has been filled by Miocene marine sediments to Pliocene silty clay marine sediments (Fais et al., 1996; Lecca, 2000). Westwards, the basement is depressed and overlain by the Pliocene and Quaternary sequence (Fais et al., 1996; Lecca, 2000). A submerged volcanic field consisting of 40 conical-shaped volcanic edifices, dated to the early Pliocene, outcrops along the shelf (Conforti et al., 2016). The transgressive deposits associated with the last sea level rise are characterised by a thin layer of coarse bioclastic sediments at the top of bedrock, as well as clays and calcareous muds along the outer shelf. In addition, there are sandy sedimentary wedges along the inner shelf composed of siliciclastic gravelly sands and calcareous bioclastic sands (Carboni et al., 1989; De Falco et al., 2008, 2010). The seabed is composed of an alternation of rocky outcrops, relict sedimentary deposits, and sands with a dominant carbonate composition (~60%) (Brambilla et al., 2019; Carboni et al., 1989; Conforti et al., 2016; De Falco et al., 2015b; De Luca et al., 2020; Lecca et al., 1983).

3. Methods and software

The main map has been produced by interpreting various data sources (Figure 1). Some data, as described below, belong to the database of the author and the Consiglio Nazionale delle Ricerche (CNR)

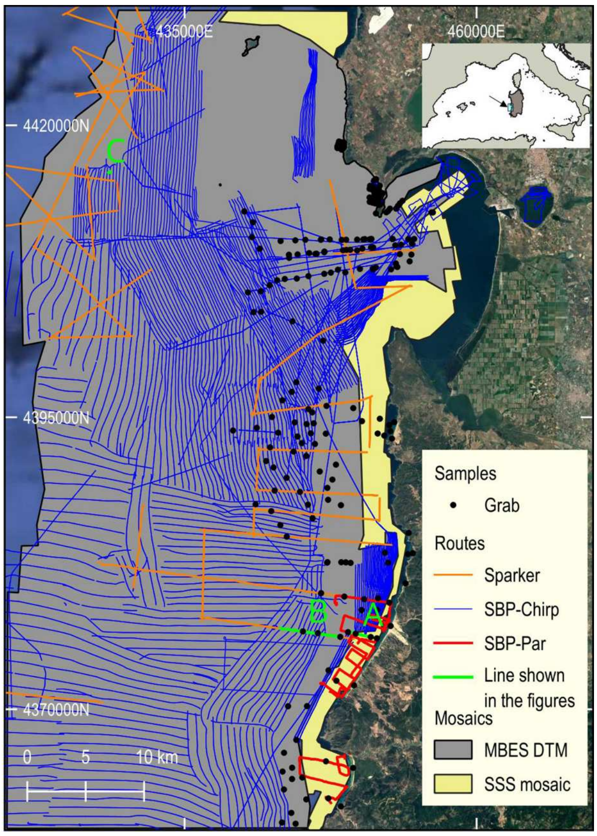

Figure 1. Locations of collected data sets: Subbottom Profiler (SBP), Multibeam Echosounder Digital Terrain Model (MBES DTM, Side-scan sonar (SSS)). The map also show the position of the line shown on Figure 3, Figure 4 and Figure 5 – Coordinate System reference: UTM zone 32 T, WGS84 datum – EPSG: 32632; linear Unit: Metre.

(Brambilla et al., 2019; Conforti et al., 2016; De Falco et al., 2003; 2008; 2010; 2015a; 2015b; 2022; 2024; Simeone et al., 2021), while others are newly acquired to improve the information and the mapping of the study area. Firstly, the coastline was derived from the 'Linea di costa marina' (DGBT 10 K rev. 2022, https://www.sardegnageoportale.it/ database access date 07/03/2024), produced by the 'Regione Autonoma della Sardegna' (RAS), and verified on the RAS-AGEA 2022 orthophoto. The orthophoto is also used as background in the 'Geolithological map' (Main map). The 'Beach systems' features referred to the 'Piano Paesaggistico Regionale (PPR, 2006)' (https://www.sardegnageoportale.it/ database access date 24/07/2024), produced by the 'Regione Autonoma della Sardegna' (RAS), integrated with detailed data produced by the authors which concern the coastal dunes (Casagrande et al., 2023).

Sea-bottom mapping was carried out by interpreting orthophotos, side-scan sonar orthomosaics, multibeam echosounder data (DTM and backscatter), seismic data, and sediment samples, which were also used as ground truth. Side-scan sonar (SSS) data were acquired in 2000 within a depth range of 10–50 m (VV.AA, 2002). Multibeam echosounder (MBES) data were collected throughout the western margin of Sardinia within the framework of the Italian projects MaGIC (Marine Geohazards along the Italian Coasts) and RITMARE, providing a comprehensive morphological definition of the mid-outer continental shelf/upper slope sectors. Data were collected during four oceanographic cruises in 2009, 2011, 2013 and 2016 using the R/V *Maria Grazia*, R/V *Urania* and R/V *Minerva uno* of the Italian National Research Council (CNR), equipped with different instruments. In the depth range 50–70 m depth range, data were acquired using the Kongsberg EM 3002D (293–307 kHz), equipped with two heads angled at approximately 33° which provided a wide swath up to a depth 150 m, a vertical resolution of 1 cm, and a footprint of 1.2–8 m for the 50–100 m depth range. The deeper sectors (70–700–800 m) were mapped using the Kongsberg EM 710 MBES. The Kongsberg EM 710 works at a frequency of 100 kHz, with a footprint of 1.2–5.7 m in a depth range of 50–100 m.

Both MBES devices also provided backscatter data which were used for interpreting the characteristics of the seabed. All data were processed using the Caris Hips and Sips software.

Finally, on the base of all MBES dataset, digital terrain models (DTMs) were produced at a 2.5 m resolution and the visualisation was obtained by using Marble Geographics Global Mapper Pro and Golden Software Surfer 10.

This new MBES dataset integrates previous data acquired along the Gulf of Oristano in 2007, using a Seabat-Reson 8111 MBES device (De Falco et al., 2010). The Reson 8111 provided data with a lower resolution which allows a DTM with a horizontal resolution of 5 m. Furthermore, a backscatter map was produced of relative backscatter intensity values (De Falco et al., 2010).

High-resolution seismic reflection profiles were collected in the study area, with a Geotech multi-tip spark array (MTSA). The Geotech MTSA source was sparking at 0.4–1 kJ, and data were processed with debias correction, filtering and gain corrections (De Falco et al., 2015a).

Furthermore, very high resolution seismic data were acquired using the sub-bottom profiler Datasonic Chirp II operating at 3.5 kHz (2.5–7 kHz). This SBP-Chirp data allowed for a greater spatial resolution (lateral resolution 0.6 m, vertical resolution 0.5 m), thus resolving more details in fine-grained superficial deposits. All seismic data were processed in order to increase the signal/noise ratio using the software Geosuite (De Falco et al., 2015a). Moreover, new seismic data were collected in 2024, from a depth of 4 m to 70 m, by a parametric sub-bottom profiler, the Innomar compact®. This SBP-par acquires multiples profiles at the same time in the range of 4–15 kHz frequencies (Figure 1).

To integrate the sedimentological database from previous surveys in the study area, new 48 sediment samples were collected with a Van Veen grab during two different survey cruises, in 2016 and 2024 (Figure 1). Sample positions were determined after the early interpretation of DTM and used as a seabed ground truth at different depths (between −85 and −5 m b.s.l). A total of 48 sediment samples were collected and analysed.

Grain-size distribution was measured using dry sieving for the gravel/sand fraction between 4000 and 90 µm at half-phi intervals. The finer fraction (<90 µm), where present, was analysed using a Galai CIS 1 laser system at 5 µm intervals (De Falco et al., 2003, 2015b; Molinaroli et al., 2009). Carbonate content was determined using a Dietrich-Fruhling calcimeter. Statistical parameters of grain size data distributions were computed using the GRADISTAT package (Blott & Pye, 2001).

Morphological analysis and interpretation of seabed and features, as well as the overlap of MBES and SSS data and sedimentological information were processed using cartographic software like Blue Marble Geographics Global Mapper and QGIS 3.34.10 'Prizren'.

All the results are stored in the UTM – WGS84 datum coordinate system.

4. Results

The geophysical and sedimentological data allowed us to map the morphological features of the seabed,

Table 1. Comparison of depths of different morphologies associated with submerged beach systems: Infralittoral Prograding Wedges (IPWs)/Submerged Depositional Terraces (SDTs) at the rollover point (ROP), barriers and paleo-dunes.

Depth (m bsl)	IPWs/SDTs (ROP)	Barriers (foot)	Paleo-dunes (foot/top)
−7		Barrier	
−12		Barrier	
−15	IPW S.Giovanni		
−26	IPW Piscinas		
−32		Barrier	Dune top
−44			Dune foot
−46	T4		
−38		Barrier	
−51	T3		
−53		Barrier	
−55	T2		
−70	T1	Barrier	
−80	T0.3		
−92	T0.2		
−115	T0.1		
−135	T0		
−125		Paleo-cliff	
−160	T-LGM		

associated with submerged coastal systems (Table 1), and geolithological features including the distribution of sediments, rocky seabed and seagrass beds. The main map shows the distribution of submerged coastal systems along the western Sardinian shelf and consists of two different maps: the 'Submerged Coastal Systems Map' and the 'Geolithological Map'. The first map (main map) focuses on submerged features of the seabed, such as barriers (paleo-shorelines), infralittoral prograding wedges (IPWs), submerged depositional terraces (SDTs), paleo-cliffs, paleo-dunes and the distribution of rocky outcrops and hard grounds. The second map (main map) adds geo-lithological contents, pointing out the distribution of seabed sediments. Furthermore, it shows the distribution of *Posidonia oceanica* (L.) Delile seagrass meadows on both sedimentary and rocky substrates.

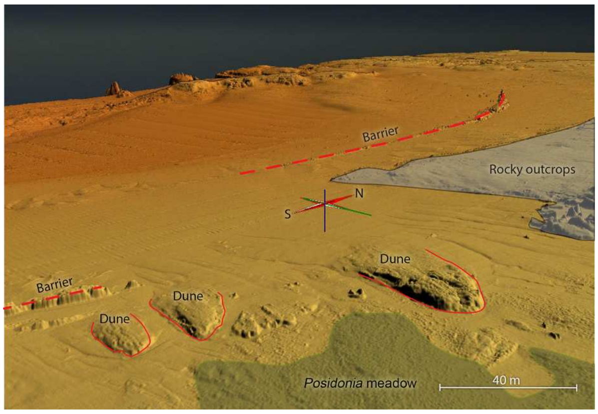

Figure 2. 3D model of a submerged coastal system (10x vertical exaggeration). The image highlighted the position of the barriers (paleo-shorelines) and the paleo-dunes.

4.1 Submerged coastal systems map

4.1.1. Barrier, dune ridge, paleo-shoreline, beachrock

Based on the mapping, it was possible to identify elongated barriers at well-defined depths. By carrying out transverse transects on the DTM and comparing them with the SBP seismic lines, it was possible to verify the nature of these barrier features and classify them as paleo-shoreline alignment (Figure 2, and Figure 3).

The barriers are arranged sub-parallel to the present coastline. Specifically, they were recognised at the depth of (top/foot of the barrier) 65 m/70, 53 m/57, 38 m/44, 32 m/35, 12 m/20 and 7 m/14 m below sea level (main map). The barriers located at the threshold of the Gulf of Oristano and at Mari Ermi (main map) were sampled. The barrier samples collected were analysed and dated using radiocarbon techniques to derive an age model that allowed us to classify the barriers as beachrocks (De Falco et al., 2015a; Vousdoukas et al., 2007; VV.AA, 2016). A particular distribution of cemented barriers was observed at the threshold of the Gulf of Oristano. Here the barriers were found at constant elevations, in a range between – 37 m and – 18 m, with a distance of ~300 m between each single barrier (De Falco et al., 2015a). The longest barrier extends for ~8 km with a width of ~130 m. The barriers are composed of mixed cemented bioclastic/siliciclastic medium sands and siliciclastic sandy gravels (De Falco et al., 2015a). Other beachrocks are present in the front of

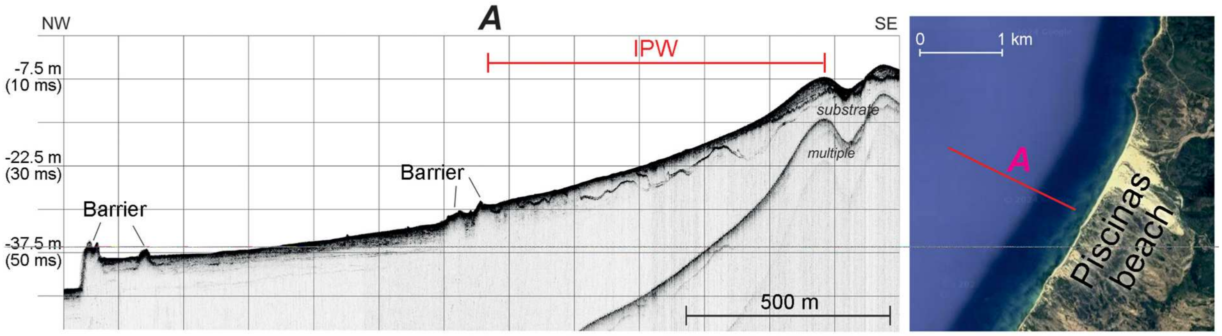

Figure 3. Parametric Subbottom Profiler (SBP-Par) seismic line with barriers and present-day infralittoral prograding wedge (IPW).

the beach of Mari Ermi. This area is characterised by the presence of a series of barriers, oriented subparallel to the present-day coastline, located between the depths of – 21 m and – 9 m b.s.l. (main map). The deepest beachrocks consist of a series of three main barriers, located between the depths of – 21 m and – 16 m, at about 1400 m from the present shoreline. The bottom of the deeper barrier is located at a depth of 21 m, while the tops are at about – 14 m, – 12 m and – 13 m, respectively. The orientation of this barrier is NW-SE and its length is about 2 km. Another shallow barrier runs parallel to the coast for about 3 km, from the north of Mari Ermi beach to the north of Is Arutas beach, at about 800 m from the shoreline. The bottom of the barrier is at a depth of 13.5 m, while the top reaches a depth of 9 m in the sector in front of Mari Ermi and 12.5 m in the sector north of Is Arutas (Simeone et al., 2021).

Other beachrocks have been identified and mapped through bibliographic analysis (VV.AA, 2016), along the Sinis coast, from Seu beach towards San Giovanni di Sinis.

An isolated beachrock was mapped about 500 m SW of the San Giovanni tower, at a depth of about – 5 m. Towards the north, the outcrop disappears under the sediments of the submerged beach of San Giovanni di Sinis (VV.AA, 2016).

To the south of San Marco cape, elongated N-S outcrops, clearly visible down to a depth of about – 30/−35 m, are recognised as paleo-shorelines (Carboni et al., 1989; Lecca, 2000).

Another outcrop has been mapped south of Isola Mal di Ventre at a depth of about 5–10 m, extending in a NE-SW direction (VV.AA, 2016).

4.1.2. Paleo-dunes

At a depth of about – 35 m, in front of Piscinas Beach, three main lithified parabolic structures were mapped. The structures are ∼350 m, ∼440 m and ∼850 m long respectively and rise about 8 m (from about – 44 m to – 32.5 m) from the seabed (Figure 2, main map). These structures follow a NWW-SEE orientation. These features were classified as a submerged dune system as they have similar shapes and orientations to the present-day dune system at Piscinas Beach (Casagrande et al., 2023).

4.1.3. Infralittoral prograding wedge (IPW)

Present-day IPWs were found at San Giovanni beach and at Piscinas beach (Figure 3).

In San Giovanni beach the IPW is located about 800 m from the coast, the rollover point (ROP) depth changes between – 15 m and – 18.2 m, the top is between – 14.7 m and – 17 m and the bottom lies between – 15 m and – 19 m. At Piscinas beach, the IPW is located at a distance of about 800–1200 m from the present shoreline, the rollover point (ROP) depth is about – 26.4 m, the top is at about – 26 m and the bottom at – 27.5 m. The rollover point refers to the location on a depositional feature, such as the IPWs or the SDTs, where the surface slope changes from a relatively steep forward slope (seaward or downslope) to a gentler backward slope (landward). On the main map, the IPWs were drawn at the rollover point (ROP) of the transverse profile (Budillon et al., 2022).

4.1.4. Submerged depositional terrace (SDT)

The map shows a series of submerged depositional terraces at different depths (Table 2, main map), characterised by flat or gently sloping surfaces ranging from 0.5–2.7 degrees. These terraces are recognised and classified according to depth as T-LGM, T0, T0.1, T0.2, T0.3, T1, T2, T3 and T4 (Table 2, main map). The structures are predominantly NW-SE oriented, except for T0.2, which is located off Piscinas Beach, sub-parallel oriented to the present coastline (Figure 4). The edge was drawn at the ROP of the transversal profile of the terraces (Budillon et al., 2022).

4.1.5. Paleo-cliff

Submerged paleo-cliffs were mapped in the northwestern sector of the map area. The edge of the cliffs is located at the present depth of – 125 m, which is consistent with global paleo-sea level during the LGM (Figure 5). For mapping purposes, paleo-cliffs were considered to be those structures with slopes greater than 20°, where the presence of an underlying erosional paleo-platform was evident.

4.2 Geolithological map

4.2.1. Surface sediments

By interpreting the multi-beam echosounder (MBES) backscatter and side-scan sonar (SSS) orthomosaics, it was possible to identify areas of different sediment grain sizes based on the acoustic response of the seafloor (De Falco et al., 2010). These areas were further validated through analysis of sediment samples according to the Folk and Ward (1957) classification (gravel, sand and silt). The map shows four different

Table 2. Parameters measured on Submerged Depositional Terraces (SDT): top and depth quotes, depth of the rollover point (ROP), average slope expressed in degrees.

SDT name	Edge ÷ Base depth (m)	ROP depth (m)	Slope (°)
T LGM	150 ÷ 200	160	1.7
T 0	134 ÷ 145	135	1.1
T 0.1	112 ÷ 125	115	1.0
T 0.2	83 ÷ 100	92	1.5
T 0.3	73 ÷ 83	80	2.7
T 1	67 ÷ 77	70	0.5
T 2	52 ÷ 63	55	1.3
T 3	48 ÷ 55	51	1.3
T 4	43 ÷ 47	46	1.5

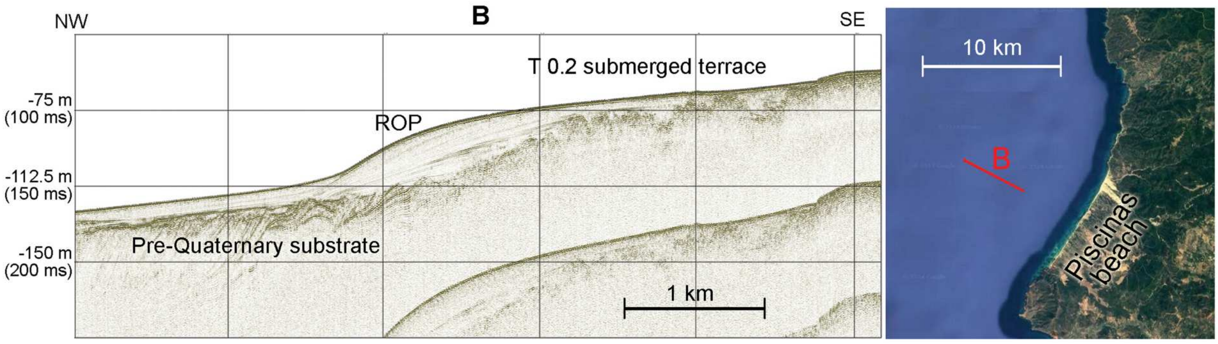

Figure 4. SPARKER seismic line, detail of T 0.2 submerged terrace with the rollover point (ROP).

sediment area of Very fine sand, Fine sand, Medium-fine sand, Coarse and gravelly sand. Medium-fine sands are mainly distributed between the submerged beach and the inner shelf up to a depth of about – 30 m. Then, at depths between about – 30 and – 60 m, coarse relict sediments (coarse sand) with a predominantly siliciclastic composition are present (Brambilla et al., 209; De Falco et al., 2015b). Among the coarse sediments, there are patches of fine sands with a mixed carbonate–siliciclastic composition (De Falco et al., 2015b). In the central sector of the map, at depths between about – 50 and – 125 m, on the outer shelf, very fine sands with a mixed carbonate–siliciclastic composition are found.

4.3.1. Rocky outcrops/hard ground

Outcrops of undifferentiated rocky substrate were recognised and mapped by interpreting the DTM coupled with seismic data. Rocky outcrops are present in the northern sector of the study area, mainly between 50 and 150 m depth, where they cover almost half of the total surface surveyed (De Falco et al., 2024). Furthermore, the rocky outcrops are present in continuity with the rocky promontories distributed along the coast of the study area (main map). They are also clearly visible in the central part of the map at a depth of about 150 m (De Falco et al., 2024). The total surface area shown on the map was estimated to be approximately 643 km^2.

4.3. *Posidonia oceanica* distribution

The *Posidonia oceanica* (L.) Delile seagrass meadows were mapped by interpreting both SSS orthomosaic (VV.AA, 2002) and MBES DTM. The upper limits of the meadow were also verified with orthophotos. The image analysis also allowed the separation of *Posidonia* on sedimentary surfaces and on hard ground surfaces.

The *Posidonia* meadow is mainly present in the northern sector, in the central sector of the map and in the Gulf of Oristano. The meadow extends from a few metres water depth down to a depth of about – 35 m b.s.l..

5. Discussion

The mapped submerged coastal systems, found at different depths, suggest that the last sea-level rise, since the LGM, was characterised by alternating phases of low and high rates of rise of sea level. During the periods of low sea-level rates, the coastal systems were formed, while during phases of fast rise of sea level, the coastal systems were submerged in the continental shelf, leading, in some cases, to the formation of overstepped barriers (De Falco et al., 2015a). This variability is attributed to climate changes that alternated phases of rapid glacier melt, characterised by accelerated SLR, known as meltwater pulses

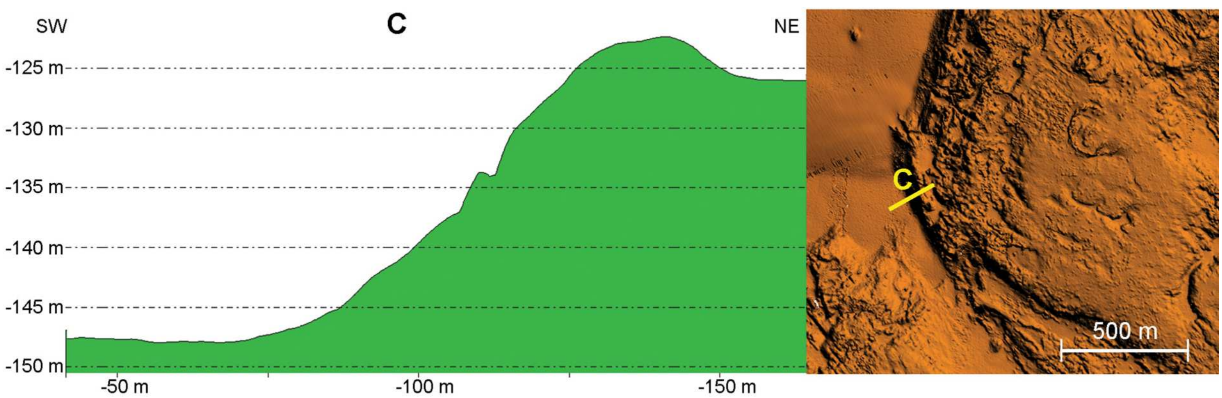

Figure 5. Profile and position of an example of a paleo-cliff.

(MWPs), with phases of slower, progressive northern hemisphere glaciers melt (Blanchon, 2011; Fairbanks, 1989; Liu & Milliman, 2004; Velay-Vitow et al., 2014). Even in the Mediterranean the response of SLR is evident (Lambeck et al., 2004, 2011, 2014) but the SRL is mainly linked to lake drainage and not directly by the glacier melt (Gregoire et al., 2012; Harrison et al., 2019; Smith et al., 2011).

The formation and evolution of submerged coastal systems were considered in relation to the current coastal systems of the study area. Dune beach systems, with associated IPWs, barrier-lagoon systems, pocket beaches and geologically controlled beaches are present along the central-western coast of Sardinia (De Falco et al., 2022). Specifically, two main IPWs systems were mapped: Piscinas beach, where the IPW was found at about 800–1200 m from the shoreline with the ROP depth about – 26.4 m and San Giovanni beach, where the IPW is located about 800 m from the coast and the ROP depth is – 15 m/−18 m. The ROP depth values of the current IPWs can be taken as reference values to relate SDTs and submerged barriers. In fact the current IPWs can be considered as a model for the SDTs and therefore useful for the recognition of paleo-beach systems, correlated with SLR phases during the last eustatic cycle, from the LGM to the present (Budillon et al., 2022; Chiocci & Orlando, 1996; Hernández-Molina et al., 2000), and in particular during stillstands after meltwater pulses MWP-1A and the present day (De Luca et al., 2025).

The submerged depositional terrace (SDT) attributable to LGM (T-LGM), mainly highlighted in the NW sector of the map, is found at a depth of about – 160 m and it can be related to the paleo-IPWs of the LGM (about 21 ka BP). Apparently, there are no evident morphologies referable to a barrier, but this morphology can be associated with the edge of the submerged cliffs, located at a depth of – 125 m (mean global sea level at the LGM). The cliffs, formed over a paleo-rocky coast, play a geological control for the terrace T-LGM (Chiocci et al., 2002).

The terraces T0.1 (−115 m), T0.2 (−92 m) and, especially, T0.3 (−80 m), deserve special attention. In fact, their positions can be associated with the barrier (paleo-shoreline) located at ∼65 m depth (Figure 4, main map). This barrier is clearly visible in the DTM represented by parabolic morphology extending for about 9.4 km in length, with a width of about 300 m. The SDTs T0.1, T0.2 and T0.3 are 2–7 km distant from the barrier. Considering their location and elevation, these submerged coastal systems are interpreted as formed during a sea level stillstand associated to the Younger Dryas period, between the MWP-1A and MWP-1B (Liu & Milliman, 2004), as evident also in the Mediterranean (De Luca et al., 2025; Zecchin et al., 2015).

This short cold climate period, which covered a time span about 1300 ± 70 years, is dated between 12.9 and 11.6 ka BP, at the end of the Pleistocene (Bard et al., 2010; Muscheler et al., 2008; Velay-Vitow et al., 2014). Global and Mediterranean sea-level curve models place the Younger Dryas coastline to a depth of – 65/−60 m below present sea level (De Luca et al., 2025 Harrison et al., 2019; Lambeck et al., 2014;; Liu & Milliman, 2004; Storms et al., 2008).

The relatively long period of sea-level stability during the Younger Dryas phase is further confirmed by the stratigraphy of the SDT T0.2 visible in the seismic line in Figure 4, where the clinoforms prograding on the acoustic basement are evident.

At shallower depths, the submerged coastal depositional systems are characterised by SDTs (T1, T2, T3 and T4) with a less evident morphological expression, and a set of overstepping barriers at a depth between 50 and 17 m. Barrier morphologies with the related slightly accentuated SDTs T1, T2 T3 and T4, can therefore be associated with fluctuations in the rate of Holocene sea-level rise over the past ∼11 kyr up to about ∼8 ka BP. Indeed, variations of sea-level rise rate is one of the main processes that lead to the formation of barriers (Swift, 1975), and rapid increases in sea level can cause a barrier to break or drowned (Carter et al., 1989; De Falco et al., 2015b; Lorenzo-Trueba & Ashton, 2014; Storms & Swift, 2003).

Particular attention on the map can be given to the submerged beach system in front of the Piscinas-Scivu beach (main map). In this area it is possible to identify the coastline and the current IPW. The wedge is located at a depth of about 26 m, at a distance of about 1200 m from the current coastline. Moving offshore at a depth of 34–32 m, we find the first barrier, oriented NNE-SSW, at a distance of about 1600 m from the coastline. Subsequently, at a depth of 38–43 m, we find a second barrier, much more evident than the previous one, with the same alignment, located 2600 m from the current coastline. In the northern sector of the map, in particular on the beach of Mari Ermi, other barriers are located at shallower depths between – 20 m and – 5 m of depth. Those barriers can be tentatively related to further fluctuations of sea level rise rates during the last ∼8 kyr. However, for these barriers, the related SDTs are not evident.

6. Conclusions

The map of submerged coastal systems along the western Sardinian shelf has been produced at a scale of 1:100,000. The map provides information on the position and distribution of morphologies associated with paleo-coastal systems that developed during the late Pleistocene-Holocene sea-level rise.

The map provides new insights into the distribution of submerged coastal systems on the western Sardinian shelf. All the elements and characteristics of the mapped seabed are related to the transition of the last eustatic cycle, starting from the Last Glacial Maximum (LGM), when the sea level was at its lowest, around – 125 m. The submerged beach systems are found at depths that are consistent with what has been described by various authors in models of sea-level rise (De Luca et al., 2025 Harrison et al., 2019; Lambeck et al., 2014;; Liu & Milliman, 2004; Storms et al., 2008), both globally and in the Mediterranean, taking into account the timing of meltwater pulses. In particular, a clear submerged coastal system was mapped at a depth of – 65 m, suggesting a link with the Youger Dryas period (12.9 - 11.6 ka BP; Bard et al., 2010).

Software

All seismic data were processed using the Geosuite, Innomar Ses-2000 and Ise 2.9.5 software. The following software were used for multibeam data processing, digital terrain model analysis and final map production: Caris Hips and Sips, Marble Geographics Global Mapper Pro 24.1, Golden Software Inc. Surfer 17, QGIS 3.34.10 LTR 'Prizren', Microsoft Office 365. All software are licensed to the National Research Council (CNR) or are Open Source.

Geo-localization information

The map provided area is located at following coordinates UTM 32N WGS84 datum (EPSG 32632):

– below left corner: 419921 E; 43539804 N
– above right corner: 465266 E; 4429804 N.

Coordinate System reference:
UTM zone 32 T, WGS84 *datum* (EPSG 32632); Geographic WGS84 *datum* (EPSG 4326).

The coastline map refers to the 1:10,000 scale shapefile '*Linea di costa marina*' (DGBT 10 K rev. 2022), produced by the *Regione Autonoma della Sardegna* (RAS), verified and modified on the basis of the RAS-AGEA 2022 orthophoto. The orthophoto is also used as background in the 'Geolithological map'.

The 'Beach system' features referred to the '*Piano Paesaggistico Regionale* (PPR, 2006)' produced by the *Regione Autonoma della Sardegna* (RAS), integrated with new data for which concern the coastal dunes.

Depth lines are referred to the 1:100,000 scale Nautical map no. 47 '*Dall'Isola di San Pietro a Capo S. Marco*' (ISBN: IDRO47) produced by the '*Istituto Idrografico della Marina Italiana*' (IIMI), integrated and modified with the MBES DTM contour analysis.

Disclosure statement

No potential conflict of interest was reported by the author(s).

Funding

Research activity funded by: PRIN2022 – Bando 2022 Prot. 2022P9N4EA – 'Beach-dune Systems in a Transgressive Domain: Evolution, Morphodynamics and Future Perspectives'. Finanziato dall'Unione europea – Next Generation EU, Missione 4 Componente 1 – CUP: B53D23007390006. Progetto CARG (CARtografia Geologica), Carta Geologica d'Italia alla scala 1:50.000, F. 546 'Guspini'. Kalb C. Research Fellow funded by PRIN2022 – Bando 2022 Prot. 2022P9N4EA – 'Beach-dune Systems in a Transgressive Domain: Evolution, Morphodynamics and Future Perspectives', Finanziato dall'Unione europea – Next Generation EU, Missione 4 Componente 1 CUP: B53D23007390006.

Data availability statement

Data available on request from the authors. The data that support the findings of this study are available from the corresponding author, C. Kalb (claudio.kalb@ias.cnr.it), upon reasonable request.

ORCID

Claudio Kalb http://orcid.org/0009-0007-0962-9226
Duccio Bertoni http://orcid.org/0000-0003-4323-2437
Annelore Bezzi http://orcid.org/0000-0001-5332-2052
Giulia Casagrande http://orcid.org/0009-0008-0909-4986
Alessandro Conforti http://orcid.org/0000-0003-0758-4611
Giacomo Deiana http://orcid.org/0000-0002-7019-9153
Giorgio Fontolan http://orcid.org/0000-0001-6080-288X
Marco Frau http://orcid.org/0009-0001-6102-1038
Antonio Funedda http://orcid.org/0000-0002-4624-1606
Davide Martinucci http://orcid.org/0000-0001-8969-099X
Paolo Emanuele Orrù http://orcid.org/0000-0002-2394-3154
Simone Simeone http://orcid.org/0000-0003-3005-3675
Giovanni De Falco http://orcid.org/0000-0002-4087-2933

References

Bard, E., Hamelin, B., & Delanghe, D. (2010). Deglacial meltwater pulse 1B and younger Dryas sea levels revisited with boreholes at Tahiti. *Science*, *327*(5970), 1235–1237. https://doi.org/10.1126/science.1180557

Blanchon, P. (2011). Meltwater pulses. In D. Hopley (Ed.), *Encyclopedia of modern coral reefs. Encyclopedia of earth sciences series* (pp. 683–690). Springer. https://doi.org/10.1007/978-90-481-2639-2_232

Blott, S. J., & Pye, K. (2001). GRADISTAT: A grain size distribution and statistics package for the analysis of unconsolidated sediments. *Earth Surface Processes and Landforms*, *26*(11), 1237–1248. https://doi.org/10.1002/esp.261

Brambilla, W., Conforti, A., Simeone, S., Carrara, P., Lanucara, S., & De Falco, G. (2019). Data set of submerged sand deposits organised in an interoperable spatial data infrastructure (Western Sardinia, Mediterranean Sea). *Earth System Science Data*, *11*(2), 515–527. https://doi.org/10.5194/essd-11-515-2019

Budillon, F., Amodio, S., Alberico, I., Contestabile, P., Vacchi, M., Innangi, S., & Molisso, A. (2022). Present-day infralittoral prograding wedges (IPWs) in Central-Eastern Tyrrhenian Sea: Critical issues and challenges to their use as geomorphological indicators of sea level. *Marine Geology*, *450*, 106821. https://doi.org/10.1016/j.margeo.2022.106821

Budillon, F., Senatore, M. R., Insinga, D., Iorio, M., Lubritto, C., Roca, M., & Rumolo, P. (2012). Late Holocene sedimentary changes in shallow water settings: The case of the Sele River offshore in the Salerno Gulf (South-Eastern Tyrrhenian Sea, Italy). *Rendiconti Lincei*, *23*, 25–43. https://doi.org/10.1007/s12210-012-0164-6

Carboni, S., Lecca, L., & Ferrara, C. (1989). La discordanza versiliana sulla piattaforma occidentale della Sardegna. *Bollettino Società Geologica Italiana*, *108*, 503–519.

Carter, R. W. G., Forbes, D. L., Jennings, S. C., Orford, J. D., Shaw, J., & Taylor, R. B. (1989). Barrier and lagoon coast evolution under differing relative sea-level regimes: Examples from Ireland and Nova Scotia. *Marine Geology*, *88*, 221–242.

Casagrande, G., Bezzi, A., Fracaros, S., Martinucci, D., Pillon, S., Salvador, P., Sponza, S., & Fontolan, G. (2023). Quantifying transgressive coastal changes using UAVs: Dune migration, overwash recovery, and barrier flooding assessment and interferences with human and natural assets. *Journal of Marine Science and Engineering*, *11*, 1044. https://doi.org/10.3390/jmse11051044

Casalbore, D., Romagnoli, C., Adami, C., Bosman, A., Falese, F., Ricchi, A., & Chiocci, F. L. (2018). Submarine depositional terraces at Salina Island (Southern Tyrrhenian Sea) and Implications on the Late-Quaternary evolution of the insular shelf. *Geosciences*, *8*, 20. https://doi.org/10.3390/geosciences8010020

Chiocci, F. L., D'Angelo, S., Romagnoli, C., Ricci Lucchi, F., & SDT Working Group (2002). Submerged depositional terraces along the Italian coasts – conclusion. *Memorie Descrittive della Carta Geologica d'Italia,, LVIII*, 111–116.

Chiocci, F. L., & Orlando, L. (1996). Lowstand terraces on Tyrrhenian Sea steep continental slopes. *Marine Geology*, *134*, 127–143. https://doi.org/10.1016/0025-3227(96)00023-0

Chiocci, F. L., & Romagnoli, C. (2004). Submerged depositional terraces in the Aeolian Islands (sicily). In F. L. Chiocci, S. D'Angelo, & C. Romagnoli (Eds.), *Atlas of submerged depositional terraces along the Italian coasts. Memorie descrittive della carta geologica d'Italia, LVIII* (pp. 49–64). ISPRA - Servizio Geologico d'Italia.

Conforti, A., Budillon, F., Tonielli, R., & De Falco, G. (2016). A newly discovered Pliocene volcanic field on the western Sardinia continental margin (western Mediterranean). *Geo-Marine Letters*, *36*(1), 1–14. https://doi.org/10.1007/s00367-015-0428-0

De Falco, G., Antonioli, F., Fontolan, G., Lo Presti, V., Simeone, S., & Tonielli, R. (2015a). Early cementation and accommodation space dictate the evolution of an overstepping barrier system during the Holocene. *Marine Geology*, *369*, 52–66. https://doi.org/10.1016/j.margeo.2015.08.002

De Falco, G., Baroli, M., Cucco, A., & Simeone, S. (2008). Intrabasinal conditions promoting the development of a biogenic carbonate sedimentary facies associated with the seagrass *Posidonia oceanica*. *Continental Shelf Research*, *28*(6), 797–812.

De Falco, G., Budillon, F., Conforti, A., Di Bitetto, M., Di Martino, G., Innangi, S., Simeone, S., & Tonielli, R. (2015b). Sorted bedforms over transgressive deposits along the continental shelf of western Sardinia (Mediterranean Sea). *Marine Geology*, *359*, 75–88.

De Falco, G., Carannante, A., Del Vais, C., Gasperini, L., Pascucci, V., Sanna, I., Simeone, S., & Conforti, A. (2022). Evolution of a single incised valley related to inherited geology, sea level rise and climate changes during the Holocene (Tirso river, Sardinia, western Mediterranean Sea). *Marine Geology*, *451*. https://doi.org/10.1016/j.margeo.2022.106885

De Falco, G., Conforti, A., Di Martino, G., Innangi, S., Simeone, S., Tonielli, R., & Budillon, F. (2024). Geohazard features of the western Sardinia. *Journal of Maps*, *20*(1), https://doi.org/10.1080/17445647.2024.2347890

De Falco, G., Molinaroli, E., Baroli, M., & Bellacicco, S. (2003). Grain size and compositional trends of sediments from *Posidonia oceanica* meadows to beach shore, Sardinia, western Mediterranean. *Estuarine, Coastal and Shelf Science*, *58*, 299–309. https://doi.org/10.1016/S0272-7714(03)00082-9

De Falco, G., Tonielli, R., Di Martino, G., Innangi, S., Simeone, S., & Parnum, I. M. (2010). Relationships between multibeam backscatter, sediment grain size, and *Posidonia oceanica* seagrass distribution. *Continental Shelf Research*, *30*, 1941–1950.

Deiana, G., Antonioli, F., Moretti, L., Orrù, P. E., Randazzo, G., & Lo Presti, V. (2021). MIS 5.5 highstand and future sea level flooding at 2100 and 2300 in tectonically stable areas of Central Mediterranean Sea: Sardinia and the Pontina Plain (Southern Latium), Italy. *Water*, *13*, 2597. https://doi.org/10.3390/w13182597

De Luca, M., Casini, L., Cossu, G., De Falco, G., Gamberi, F., Marras, P., Santonaso, A., Stelletti, M., & Pascucci, V. (2025). Geomorphology of the northeast Sardinian continental shelf between Olbia and Posada (Italy). *Journal of Maps*, *21*(1). https://doi.org/10.1080/17445647.2024.2446249

De Luca, M., Chaiallah, A., Andreucci, S., Cossu, G., Santonastaso, A., Sechi, D., Stelletti, M., & Pascucci, V. (2020). Seafloor Map of the Alghero Bay (Sardinia, Italy). *Journal of Maps*, *16*(2), 669–679. https://doi.org/10.1080/17445647.2020.1805808

Fairbanks, R. (1989). A 17,000-year glacio-eustatic sea level record: Influence of glacial melting rates on the Younger Dryas event and deep-ocean circulation. *Nature*, *342*, 637–642. https://doi.org/10.1038/342637a0

Fais, S., Klingele, E. E., & Lecca, L. (1996). Oligo-Miocene half graben structure in Western Sardinian Shelf (western Mediterranean): reflection seismic and aeromagnetic data comparison. *Marine Geology*, *133*(3/4), 203–222. https://doi.org/10.1016/0025-3227(96)00030-8

Fernàndez-Salas, L. M., Dabrio, C. J., Goy, J. L., Díaz del Río, V., Zazo, C., Lobo, F. J., Sanz, J. L., & Lario, J. (2009). Land–sea correlation between late Holocene coastal and infralittoral deposits in the SE Iberian Peninsula (Western Mediterranean). *Geomorphology*, *104*, 4–11. https://doi.org/10.1016/j.geomorph.2008.05.013

Field, M. E., & Roy, P. S. (1984). Offshore transport and sand-body formation: evidence from a steep, high-energy shoreface, South-eastern Australia. *Journal of Sedimentary Research*, *54*(4), 1292–1302. https://doi.org/10.1306/212F85C1-2B24-11D7-8648000102C1865D

Firetto Carlino, M., Di Stefano, A., & Budillon, F. (2012). Seismic facies and seabed morphology in a tectonically controlled continental shelf: The Augusta Bay (offshore eastern Sicily, Ionian Sea). *Marine Geology*, *335*, 35–51. https://doi.org/10.1016/j.margeo.2012.10.009

Folk, R. L., & Ward, W. C. (1957). Brazos River bar (Texas); a study in the significance of grain size parameters. *Journal of Sedimentary Research*, *27*(1), 3–26. https://doi.org/10.1306/74D70646-2B21-11D7-8648000102C1865D

Geletti, R., Zgur, F., Del Ben, A., Buriola, F., Fais, S., Fedi, M., Forte, E., Mocnik, A., Paoletti, V., Pipan, M., Ramella, R., Romeo, R., & Romi, A. (2014). The messinian salinity crisis: New seismic evidence in the West-Sardinian margin and Eastern Sardo-Provençal basin (West Mediterranean Sea). *Marine Geology*, *351*, 76–90. https://doi.org/10.1016/j.margeo.2014.03.019

Gregoire, L., Payne, A., & Valdes, P. (2012). Deglacial rapid sea level rises caused by ice-sheet saddle collapses. *Nature*, *487*, 219–222. https://doi.org/10.1038/nature11257

Hampson, G. J., & Storms, J. E. A. (2003). Geomorphological and sequence stratigraphic variability in wave-dominated, shoreface-shelf parasequences. *Sedimentology*, *50*, 667–701.

Harrison, S., Smith, D. E., & Glasser, N. F. (2019). Late Quaternary meltwater pulses and sea level change. *Journal of Quaternary Science*, *34*, 1–15. https://doi.org/10.1002/jqs.3070

Hernández-Molina, F. J., Fernández-Salas, L. M., Lobo, F., Somoza, L., Díaz-del-Río, V., & Alveirinho Dias, J. M. (2000). The infralittoral prograding wedge: A new large-scale progradational sedimentary body in shallow marine environments. *Geo-Marine Letters*, *20*(2), 109–117. https://doi.org/10.1007/s003670000040

Lambeck, K., Antonioli, F., Anzidei, M., Ferranti, L., Leoni, G., Scicchitano, G., & Silenzi, S. (2011). Sea-level changes along the Italian coast during the Holocene and a projection for the future. *Quaternary International*, *232*, 250–257. https://doi.org/10.1016/j.quaint.2010.04.026

Lambeck, K., Antonioli, F., Purcell, A., & Silenzi, S. (2004). Sea-level changes along the Italian coast for the past 10,000 yr. *Quaternary Science Reviews*, *23*, 1567–1598. https://doi.org/10.1016/j.quascirev.2004.02.009

Lambeck, K., & Bard, E. (2000). Sea-level change along the French Mediterranean coast since the time of the Last Glacial Maximum. *Earth and Planetary Science Letters*, *175*, 203–222.

Lambeck, K., Rouby, H., Purcell, A., Sun, Y., & Sambridge, M. (2014). Sea level and global ice volumes from the Last Glacial Maximum to the Holocene. *PNAS*, *111*(43), 15296–15303. https://doi.org/10.1073/pnas.1411762111

Lecca, L. (2000). La piattaforma continentale miocenico–quaternaria del margine occidentale sardo: Blocco diagramma sezionato. *Rendiconti del Seminario della Facoltà di Scienze dell'Università di Cagliari*, *70*(1), 49–70.

Lecca, L., Scarteddu, R., & Sechi, F. (1983). La piattaforma continentale sarda da Capo Mannu a Capo Marrargiu. *Bollettino Società Geologica Italiana*, *102*, 57–86.

Liu, J. P., & Milliman, J. D. (2004). Reconsidering Meltwater pulses 1A and 1B: Global impacts of rapid sea-level rise. *Journal of Ocean University of China (Oceanic and Coastal Sea Research)*, *3*(2), 183–190.

Lorenzo-Trueba, J., & Ashton, A. D. (2014). Rollover, drowning, and discontinuous retreat: Distinct modes of barrier response to sea-level rise arising from a simple morphodynamic model. *Journal of Geophysical Research: Earth Surface*, *119*, 779–801. https://doi.org/10.1002/2013JF002941

Massari, F., & Chiocci, F. L. (2006). Biocalcarenite and mixed cool-water prograding bodies of the Mediterranean Pliocene and Pleistocene: Architecture, depositional setting and forcing factors. *Geological Society, London, Special Publications*, *255*, 95–120. https://doi.org/10.1144/GSL.SP.2006.255.01.08

Molinaroli, E., Guerzoni, S., De Falco, G., Sarretta, A., Cucco, A., Como, S., Simeone, S., Perilli, A., & Magni, P. (2009). Relationships between hydrodynamic parameters and grain size in two contrasting transitional environments: The Lagoons of Venice and Cabras Italy. *Sedimentary Geology*, *219*, 196–207.

Muscheler, R., Kromer, B., Björck, S., Svensson, A., Friedrich, M., Kaiser, K. F., & Southon, J. (2008). Tree rings and ice cores reveal ^{14}C calibration uncertainties during the Younger Dryas. *Nature Geoscience*, *1*, 263–267. https://doi.org/10.1038/ngeo128

Pepe, F., Bertotti, G., Ferranti, L., Sacchi, M., Collura, A. M., Passaro, S., & Sulli, A. (2014). Pattern and rate of post-20 ka vertical tectonic motion around the Capo Vaticano Promontory (W Calabria, Italy) based on offshore geomorphological indicators. *Quaternary International*, *332*, 85–98. https://doi.org/10.1016/j.quaint.2013.11.012

Pomar, L., & Tropeano, M. (2001). The Calcarenite di Gravina formation in Matera (Southern Italy): new insights for coarse-grained, large-scale, cross-bedded bodies encased in offshore deposits. *AAPG Bulletin*, *85*(4), 661–689. https://doi.org/10.1306/8626C979-173B-11D7-8645000102C1865D

Reading, H. G., & Collison, J. D. (1996). Clastic coasts. In H. G. Reading (Ed.), *Sedimentary environments: Processes, facies and stratigraphy* (3rd edn). Blackwell Science, 154–231.

Romagnoli, C. (2004). Submerged depositional terraces around Linosa Island (Sicily Channel). In *APAT – Atlante dei Terrazzi Deposizionali sommersi. Memorie descrittive della Carta Geologica D'Italia, LVIII* (pp. 71–74). ISPRA - Servizio Geologico d'Italia.

Sage, F., Von Gronefeld, G., Déverchère, J., Gaullier, V., Maillard, A., & Gorini, C. (2005). Seismic evidence for Messinian detrital deposits at the western Sardinia margin, northwestern Mediterranean. *Marine and Petroleum Geology*, *22*(6-7), 757–773. https://doi.org/10.1016/j.marpetgeo.2005.03.007

Simeone, S., Palombo, L., Molinaroli, E., Brambilla, W., Conforti, A., & De Falco, G. (2021). Shoreline response to wave forcing and sea level rise along a geomorphological complex coastline (Western Sardinia, Mediterranean Sea). *Applied Sciences*, *11*, 4009. https://doi.org/10.3390/App11094009

Smith, D. E., Harrison, S., Firth, C. R., & Jordan, J. T. (2011). The early Holocene sea level rise. *Quaternary Science Reviews*, *30*(15–16), 1846–1860. https://doi.org/10.1016/j.quascirev.2011.04.019

Storms, J. E. A., & Swift, D. J. P. (2003). Shallow marine sequences as the building blocks of stratigraphy: Insights from numerical modeling. *Basin Research*, *15*, 287–303. https://doi.org/10.1046/j.1365-2117.2003.00207.x

Storms, J. E. A., Weltje, G. J., Terra, G. J., Cattaneo, A., & Trincardi, F. (2008). Coastal dynamics under conditions of rapid sea-level rise: Late Pleistocene to Early Holocene evolution of barrier–lagoon systems on the northern Adriatic shelf (Italy). *Quaternary Science*

Reviews, *27*(11–12), 1107–1123. https://doi.org/10.1016/j.quascirev.2008.02.009

Swift, D. J. P. (1975). Tidal sand ridges and shoal retreat massifs. *Marine Geology*, *18*, 105–134.

Vacchi, M., Joyse, K. M., Kopp, R. E., Marriner, N., Kaniewski, D., & Rovere, A. (2021). Climate pacing of millennial sea-level change variability in the central and western Mediterranean. *Nature Communication*, *12*, 4013. https://doi.org/10.1038/s41467-021-24250-1

Velay-Vitow, J., Chandan, D., & Peltier, W. R. (2014). Into the Holocene, anatomy of the Younger Dryas cold reversal and preboreal oscillation. *Scientific Reports*, *14*, 3134. https://doi.org/10.1038/s41598-024-53591-2

Vousdoukas, M. I., Velegrakis, A. F., & Plomaritis, T. A. (2007). Beachrock occurrence, characteristics, formation mechanisms and impacts. *Earth-Science Reviews*, *85*, 23–46. https://doi.org/10.1016/j.earscirev.2007.07.002

VV.AA. (2002). *Mappatura delle praterie di Posidonia oceanica lungo le coste della Sardegna e delle piccole isole circostanti*. Cooperativa Nautilus di Vibo Valentia - Ministero dell'Ambiente e della Tutela del Territorio – Servizio difesa del mare 1999-2002.

VV.AA. (2016). Note illustrative della Carta Geologica d'Italia alla scala 1:50.000, F. 528 Oristano, ISPRA - Serv. Geol. d'It., Roma. https://doi.org/10.15161/oar.it/143411.

Zecchin, M., Ceramicola, S., Lodolo, E., Casalbore, D., & Chiocci, F. L. (2015). Episodic, rapid sea-level rises on the central Mediterranean shelves after the Last Glacial Maximum: A review. *Marine Geology*, *369*, 212–223. https://doi.org/10.1016/j.margeo.2015.09.002